Shape memory polymers based on uniform aliphatic urethane networks

T. S. Wilson, J. P. Bearinger, J. L. Herberg, J. E. Marion III, W. J. Wright, C. L. Evans, D. J. Maitland

January 23, 2007

Disclaimer

Shape memory polymers based on uniform aliphatic urethane networks

T S. Wilson[1], J. P. Bearinger[1], J. L. Herberg[2], J. E. Marion III[1] , W. Wright[3], C. L. Evans[2], and D. J. Maitland[1]

[1]Applied Physics and Biophysics Division, Lawrence Livermore National Laboratory, 7000 East Avenue, Livermore CA 94551.

[2]CMLS, LLNL, 7000 East Avenue, Livermore, CA 94551.

[3]Dept of Mechanical Engineering, Santa Clara University, Santa Clara, California 95053.

Correspondence to: T. S. Wilson (wilson97@llnl.gov).

ABSTRACT

Aliphatic urethane polymers have been synthesized and characterized, using monomers with high molecular symmetry, in order to form amorphous networks with very uniform supermolecular structures which can be used as photo-thermally actuable shape memory polymers (SMPs). The monomers used include hexamethylene diisocyanate (HDI), trimethylhexamethylenediamine (TMHDI), N,N,N',N'-tetrakis(hydroxypropyl)ethylenediamine (HPED), triethanolamine (TEA), and 1,3-butanediol (BD). The new polymers were characterized by solvent extraction, NMR, XPS, UV/VIS, DSC, DMTA, and tensile testing. The resulting polymers were found to be single phase amorphous networks with very high gel fraction, excellent optical clarity, and extremely sharp single glass transitions in the range of 34 to 153 °C. Thermomechanical testing of these materials confirms their excellent shape memory behavior, high recovery force, and low mechanical

hysteresis (especially on multiple cycles), effectively behaving as ideal elastomers above T_g. We believe these materials represent a new and potentially important class of SMPs, and should be especially useful in applications such as biomedical microdevices.

INTRODUCTION

Shape memory polymers (SMPs) have recently been receiving a great deal of interest in the scientific community for their use in applications ranging from light weight structures in space [1] to micro-actuators in micro-electro-mechanical systems (MEMS) [2-4]. These materials can be formed into a primary shape, reformed into a stable secondary shape, then controllably actuated to recover their primary shape. Such behavior has been reported in a wide variety of polymers including polyisoprene [5], segmented polyurethanes [6-14] and their ionomers [11], copolyesters [15, 16], ethylene-vinylacetate copolymers [17], and styrene-butadiene copolymers [18]. A comprehensive review of shape memory polymer chemistries and chain topologies has been given by Lendlein [19] and is not repeated here though the field is currently one of rapid progress.

The use of SMPs for biomedical devices is more recent [2-3, 20-21] and follows the use of shape memory alloys (SMAs), such as of nickel-titanium (Nitinol) [22]. However, SMPs have very different physical properties and some distinct advantages over the SMAs. Thermally actuated SMA shape recovery is accompanied by a moderate change in elastic modulus (10 to 80 GPa), large recovery stresses (~ 1000 MPa), and low recovery strains (< 8 %), and high thermal hysteresis. In contrast, in thermally actuated SMPs deformation is stored elastically as macromolecular chain orientation; hence, there is an entropic potential for shape recovery. Upon actuation shape recovery

is accompanied by a large change in elastic modulus (from 2 GPa to 0.002 GPa), low recovery stresses (~ 1 to 10 MPa), large recovery strains (>300%), and thermal hysteresis. SMAs are therefore more useful in actuators for which greater forces are needed and SMPs are more useful when greater shape change is required.   However, there is a large middle ground between these two types of materials for which suitable materials are scarce [23].

The focus of this work was to investigate the question of whether materials could be designed and synthesized which have mechanical properties somewhat between those previously reported for SMPs and SMAs. This was generally considered to mean increasing the modulus of the SMPs (hence increased recovery stress) with the inherent trade-off in reduced recoverable strain. Additional criteria, driven by the target application of photo-thermally actuated microdevices, includes high optical clarity, sharp and controllable actuation temperatures, low energy input to achieve actuation, and high biocompatibility and biostability for medical implants.

In recent years a large number of shape memory polymers have been developed for a myriad of applications. These have recently been reviewed with regard to the relationship between supermolecular structure and shape memory behavior [19].   Generally, thermally actuated (shape change caused by heating) SMPs can be thought of as having a morphology consisting of a shape fixing matrix phase and a shape memorizing dispersed phase.   The shape memorizing phase consists of physical (crystallinity, glassy phase, ionic or hydrogen bonding interactions) or chemical (covalent) crosslinking in the polymer, which allows the SMP to remember the primary shape. The shape fixing phase can be amorphous, or semicrystalline polymer. Above the actuation transition in the shape fixing (matrix) phase, the polymer can be deformed from its primary shape to a secondary shape by the application of stress, then locked into the secondary shape by cooling below the actuation transition. In the secondary shape, polymer chains in this matrix phase are made to go

from an equilibrium random conformation into conformations which have net orientation, decreasing the entropy of the system and requiring the application of force. Upon cooling below the actuation transition, this non-equilibrium structure is frozen. By heating through the actuation transition, recovery of the polymer from the secondary to the primary shape is driven by entropic recovery of the polymer chains in the shape fixing phase.

The design of an SMP molecular structure to achieve the desired properties requires a review of the characteristics of the different available structures and this is compiled in Table 1. A clear direction in the development of new SMPs would be in the creation of amorphous crosslinked polymers. However, even these materials may have low recovery stresses and broad glass transitions used in their actuation [24]. The achievement of high recovery stresses for these materials indicates the need for a high level of crosslinking according to the relationship between rubber plateau modulus and crosslink density as given for an ideal elastomer [25]: $E \sim n_c RT \sim RT/M_c$ where n_c is the number of crosslinks per unit volume, E is the Young's modulus, R is the gas constant, T is temperature, and M_c is the molecular weight between crosslinks. Also, since the breadth of the glass transition in a polymer can be related to the number of relaxation modes available to the polymer chains, which in turn can be related to network structure in crosslinked polymers [26], a second criteria for the new SMP was to have as regular a network chain structure as possible. This requires the formation of a network where the network chains connecting crosslink sites are as similar as possible in molecular weight and structure. Dangling chains should likewise be minimized. Therefore, the new SMPs should be based on monomers with very high structural symmetry which are incorporated into the network by end-linking.

In this work several series of network polymers were synthesized based on the selection criteria above. In addition, monomers were selected which were mutually miscible and could

produce polymers with glass transitions in the desired range of 30 to 80 °C for medical and microdevice applications. Urethane chemistry was selected due to the high degree of control over resultant polymer structure (A-B type condensation) that can be achieved. Also, aliphatic diisocyanates were chosen due to their increased biocompatibility upon biodegradation as opposed to aromatic polyurethanes [27]. Monomers chosen for the initial series (A1-A11) of SMPs were 1,6-hexamethylene diisocyanate (HDI), N,N,N',N'-tetrakis(2-hydroxypropyl)ethylenediamine (HPED), and triethanolamine (TEA). Additional series were made (B1-B7) substituting 1,3-butanediol (BD) for TEA in order to look at the effect of increasing network chain length, (C1-C6) substituting 2,2,4-trimethyl hexamethylene diisocyanate (TMHDI) for HDI to look at the effect of methyl side groups on segment dynamics, and (D) substituting isophorone diisocyanate (IPDI) or methylene bis-(4-cyclohexylisocyanate) (HMDI) in order to increase the glass transition and rubber plateau modulus due to their rigid nature. The resulting polymers were characterized by solvent extraction, NMR, XPS, UV/VIS, DSC, DMTA, and tensile testing in order to confirm their structure, thermal properties, and mechanical properties relevant to their use as shape memory materials.

EXPERIMENTAL

Materials and Sample Preparation.

All chemicals, unless otherwise stated, were purchased from Sigma-Aldrich and used as received. HDI (98%), TMHDI (TCI America, mixture of 2,2,4 and 2,4,4 isomers), HPED (98%), triethanolamine (TEA, 99%), and 1,3butanediol (1,3BD, 99% anhydrous) were used as received. Additionally, the aliphatic diisocyanates 4,4'-methylenebis(cyclohexyl isocyanate) (MCHI, 98% Lancaster) and isophorone diisocynate (IPDI, TCI America 98%) were used to look at the effect of

network chain flexibility on Tg and modulus, and to create SMPs with very high glass transitions.

Several series of polymers based on stoichiometric combinations of the above monomers were synthesized, though in this paper we will report mainly on copolymers consisting of HDI/HPED/TEA (A series), HDI/HPED/1,3BD (B series), or TMHDI/HPED/TEA (C Series). The compositions of these polymer formulations are given in Table 2. Generally, a 1 to 2% molar excess of isocyanate containing monomer was used in preparing polymers to adjust for monomer purity and residual water. The monomers were weighed in a glove box to reduce exposure to moisture, mixed for 120 seconds under high shear using a vortex mixture, vacuum degassed for 6 to 10 minutes (8 minutes typical) at 1 Torr, then cast into either cylindrical, popsicle stick, or microtensile specimens. In cases where the original monomer mixture had a tendency to phase separate, such as at high TEA or BD levels, high intensity vortex mixing at room temperature continued until the reaction had proceeded far enough that optically clear material was observed. Cylindrical specimens were made using 1ml polypropylene syringes resulting in 4.65 mm diameter by 60 mm long specimens. Popsicle sticks (1 mm by 12 mm by 80 mm) or dogbones (ASTM D638 type V specimen) were cast using an aluminum mold coated with teflon mold release (Miller-Stephenson MS-122FD). The cast parts were cured using a temperature profile of 60 minutes at room temperature, followed by a ramp to 130 °C at 30 °C /hour, followed by 1 hour at 130 °C all under a nitrogen atmosphere. Parts were allowed to cool slowly under nitrogen, removed from the molds, and stored in glass bottles or polybags under dessication.

Characterization by Swelling and Extraction.

Solvent swelling and extraction experiments were carried out on a small subset of formulations cast in the syringes in order to assess the extent of gelation of the resulting polymers.

Swelling was first carried out on example polymer formulations by placing approximately 0.20 g samples of the polymer in a 50 x quantity of the solvents phosphate buffered saline (PBS), water, ethanol, isopropanol (IPA), acetone, tetrahydrofuran (THF), and dimethyl formamide (DMF). DMF was found to be the best solvent in this series based on weight % of solvent uptake. Additional testing involved extraction of 1 gram samples of pre-dried polymer (60 minutes, 100 °C, 70 mTorr) in a 20 times excess of DMF at 100 °C for 12 hours followed by a change in solvent and an additional 12 hours at 100 °C. Extracted polymer samples were then vacuum dried (40 mTorr) at 150 °C for 71 hours which was found to produce a constant weight. To look at the possibility that moisture contributed to sample weight loss, fresh samples were weighed before and after drying for 48 hours at 150 °C and 40 mTorr.

Characterization by Nuclear Magnetic Resonance (NMR).

NMR studies were performed on example formulations of the urethanes in order to confirm compositions of the bulk polymer and look for residual functional groups after polymerization. First, HDI and HPED monomers were each dissolved in deuteriated-tetrahydrofuran (THF) and testing was carried out to verify peak position of carbon species. These tests were performed at 125.77 MHz on a Bruker Avance 500MHz spectrometer with a magnetic field of 11.74T. Both solution samples contained 25% HDI or HPED monomer and 75% THF. The solution state ^{13}C {1H} spectra were taken with a ^{13}C {1H} decoupling experiment. The ^{13}C {^{1}H} NMR data were taken with a 90 degree pulse width of 9.5µs. In these experiments, the relaxation delay was 3s and the number of acquisitions was 2,000. The ^{13}C {^{1}H}NMR data were referenced to THF at 67.57ppm and 25.37ppm.

Solid samples comprised of HDI and HPED (1:1 and 2:1 molar ratio) were analyzed using ^{13}C cross polarization magic angle spinning (CPMAS) NMR [28]. Experiments were performed on a Bruker Avance 400MHz spectrometer (9.4T, ^{13}C frequency of 100.614 MHz) using a 4 mm triple resonance CPMAS probe from Bruker. center of a 4mm Bruker rotor. Spinning rates of 12 kHz were used. The ^{13}C CPMAS spectra were taken with a cross polarization experiment [28]. The ^{13}C -NMR data were taken with a 90 degree pulse width of 4μs and X kHz 1H CW decoupling. Relaxation delays of 2s were used and the contact time was set to 1 ms. The number of acquisitions was 10,000. The ^{13}C CPMAS NMR data were referenced to glycine at 32ppm and 176.5ppm.

Characterization by X-ray Photoelectron Spectroscopy (XPS).

XPS was carried out on select samples in order to try to assess the extent of reaction and look for residual functional groups. The XPS data was collected using a Physical Electronics Quantum 2000 scanning XPS system with a focused monochromatic Al Ka x-ray (1486.7 eV) source for excitation and a spherical section analyzer. The instrument has a 16-element multichannel detection system. A 100 μm diameter x-ray beam was used for analysis. The x-ray beam is incident normal to the sample and the x-ray detector is at 45° away from the normal. The pass energy was 23.5 eV giving an overall energy resolution of 0.3 eV. The collected data were referenced to an energy scale with binding energy for Cu 2p3/2 at 932.72±0.05 eV and Au 4f7/2 at 84.01±0.05 eV. Binding energies were also referenced to the C 1s photoelectron line arising from adventitious carbon at 284.6 eV. Sensitivity factors were provided by Physical Electronics MultiPack software version 6.1A. Low energy electrons and argon ions were used for specimen neutralization. SMP samples were examined at freshly cleaved cross sections, representative of the bulk material.

Characterization by Ultraviolet, Visible, and Near-Infrared spectroscopy (UV/VIS/NIR).

UV/VIS/NIR spectroscopy was carried out on the A1 (HDI/HPED) copolymer both neat and with various concentrations of added Epolight™ 4121 (Epolin Inc., Newark, NJ) dye in the range of 2 to 108 parts per million (ppm) by weight using a Cary 300 BIO (Varian Inc., Palo Alto, CA) instrument. This was done in order to determine the specific absorbance of the polymer as a function of wavelength and determine the required amount of dye necessary for laser actuation of the shape memory relevant to use in device applications. Experiments were carried out on samples cast inside polystyrene cuvettes having a 1.0 cm pathlength. For these samples, the curing conditions for the resin was 1 hour at room temperature followed by 12 hours at 70 ºC. Corrections to the spectra were made by subtracting the absorbance from an empty cuvette cut in half, which corrects for reflections from light entering and exiting the test sample as well as 1/2 that due to the thin polystyrene cuvette.

Characterization by Differential Scanning Calorimetry (DSC).

DSC was carried out on a Perkin Elmer Diamond DSC equipped with an Intracooler 2. Samples with a mass of approximately 5 mg were cut from as polymerized test rods (stored under dessication) and placed in standard closed aluminum pans. The instrument was previously calibrated against an indium standard. The samples were loaded at room temperature, taken down to -20 °C, run in multi-ramp sequences at temperatures between -20 and 200 °C at a ramping rate of 20 °C /minute with 2 minute soaks at the end of each ramp. Glass transitions were calculated from the heat flow data using the instrument Pyris® [29] software, based on the temperature at which one half the change in the heat capacity has occurred due to the transition [30] and results are reported

for the second heating scan (Table 2). Replicate tests were only made on a few samples and indicated a standard deviation of 0.3 °C including batch to batch variation.

Characterization by Dynamic Mechanical Thermal Analysis (DMTA).

DMTA was used to determine both thermal transitions in the new SMPs as well as provide information about the resultant polymer morphology and shape-memory behavior. Measurements were made using a TA ARES-LS2 model rheometer (TA Instruments, Wilmington, DE) with TA Orchestrator [31] control software. A torsion cylinder test fixture was used with samples having a diameter of 4.65 mm diameter and 25 mm gap distance. The test atmosphere was dry air with heating by forced convection. Dynamic strain sweeps at temperature extremes (25 and 150 °C) were used to determine the limits of linear viscoelastic behavior of the neat polymer. Dynamic temperature sweep tests were then run on all samples at 6.28 radians/second (1 Hz) frequency from 25 to 150 °C, at a constant heating rate of 1˚C/minute. An initial shear strain of 0.01% was used though strain was subsequently adjusted by the control software as temperature increased to maintain a torque range of 2 to 50 gram*centimeters. Data points were collected every 15 seconds. The rheological quantities of dynamic shear storage modulus G', dynamic shear loss modulus G", and their ratio tan δ (=G"/G') were calculated using standard formulae [31]. Results shown in Table 2 are for single measurements, though replicates on select samples indicate a standard deviation for Tg of 1.5 °C and relative standard deviation of 2% for moduli values.

Characterization by Tensile Testing.

Isothermal tensile mechanical testing was carried out on the A1 sample to determine both the strength of the new SMPs and confirm their shape-memory properties. First, isothermal testing

was carried out according to ASTM D638 to failure on type V samples for select formulations at a temperature of Tg + 25 °C. Next, isothermal cyclic strain tests were run on molded "pop-sickle stick" samples, having dimensions of 60 mm x 12.5 mm x 1 mm. at Tg +25 °C. Three to five replicate tests were run for each material and method (standard tensile and cyclic).

RESULTS AND DISCUSSION

Solvent Swelling and Extraction Results.

Solvent extraction results for several urethane SMP formulations are given in Table 2. The results show that approximately 96 to 99% of the initial monomers were incorporated into the polymer network. While the composition of the soluble fraction was not explicity determined, it is likely to be a combination of impurities in the original monomers (typically 97 to 98% pure) as well as absorbed moisture. For example, samples dried under extreme conditions (150 °C, 40 millitorr, 48 hours) were found to lose from 0.4 to 1.0% of their mass, which was likely moisture. According to statistical theory for condensation polymerization [32], this indicates extents of reaction for the functional groups in the material of greater than 85%.

NMR Results.

^{13}C {^1H} NMR spectra of HDI dissolved in THF and HPED dissolved in THF are not shown. The ^{13}C {^1H}NMR spectra of the sample containing HDI shows peaks at approximately 32ppm, 43ppm, and 68ppm, which represents the three types of aliphatic carbons ($-CH_2-$). There is also a peak at 123ppm, which represents the isocyanate carbon ($-N=C=O$). The ^{13}C {^1H}NMR spectra of the sample containing HPED shows a variety peaks at 12.5-3.9ppm, 20.6-21.8ppm, and 63-68ppm, which represent aliphatic carbons in the form of CH_2 and CH_3, and the carbon for the

secondary alcohol (-HC(-OH)-), respectively.

Figure 1 shows ^{13}C CPMAS spectra for solid polymers with different concentrations of HDI and HPED. The ^{13}C CPMAS spectra of the sample containing 1:1 molar ratio of HDI/HPED show peaks at 19ppm, 20ppm, 27ppm, and 40ppm, which represents aliphatic carbons (-CH_3, -CH_2-); 54ppm and 64ppm, which represents carbon in the form of alcohol (-HC(-OH)-) and amines (>N-CH_2- and –H$_2C$-NH-); and 157ppm, which represents the carbonyl carbon in the carbamate (-O-C(=O)-NH-). The ^{13}C CPMAS spectra of the sample containing 2:1 molar ratio of HDI/HPED show peaks at 18ppm, 27ppm, 30ppm, and 41ppm, which represents aliphatic carbons (CH_3, CH_2, CH); 59ppm and 68ppm, which represents carbon in the form of alcohols and amines; and 157ppm, which represents carbon in the form of carbamate.

To determine the percentage of carbon in the form of aliphatic carbons, alcohols, amines, and carbamate, the samples were weighed, the data was normalized to the weight of the sample, and each peak in the ^{13}C CPMAS spectra were fitted to a Gaussian with a fitting program, Fityk using methods previously described [33]. Even though the ^{13}C NMR spectra of the carbons in the form of aliphatics, alcohols, and amines are difficult to separate to determine the atomic fraction of carbon in each specific species, it is possible to determine the atomic fraction of the carbonyl carbon in the form of isocyanate versus urethane. The 1:1 molar HPI/HPED sample has an atomic fraction of carbonyl carbon in the form of carbamate of 8.49 +/- 0.80%, which is in good agreement with the predicted value of 9.1% based on formulation composition. Also, the 2:1 molar HPI/HPED sample has an atomic fraction of carbonyl carbon in the form of carbamate of 15.44 +/- 1.04%, which is in good agreement with the predicted value 13.3%. This data shows both that the carbamate (urethane) linkage is being formed and there is no sign of residual isocyanate carbon, which would occur

around 122ppm. Quantitatively, these results indicate that at least 99% of the isocyanate is consumed by reaction.

XPS Results.

The elemental composition (C, O, and N) of three of the HDI/HPED/TEA copolymers as determined by XPS is given in Table 3. Carbon peaks containing the dominant methylene carbon at 284.6 eV were broad due to inclusion of amine and alcohol moieties at 286.0 and 286.5 eV respectively. Compositional results for the freshly cleaved samples are shown in Table 3. There was not enough resolution in the carbonyl carbon peak to differentiate between carbamate and isocyanate moities. Examination of peak area suggests that 5.1% of C is attributed to carbamate or isocyanate, while composition of starting materials predicts that this should place 13.3% of C at 289.6 eV. Compositionally, as TEA content increases the percent of carbamate or isocyanate on the surface decreases. This surface depletion of these groups increases as the hydrophilicity of the polymer increases.   Also, the compositions are higher in carbon and lower in nitrogen than predicted from the chemical formulations, while oxygen content is very close to that predicted.

UV/VIS Results.

All of the network urethane polymers produced in this work appeared optically clear without coloration if polymerized below approximately 150 $^{\circ}$C, though some yellowing of the materials could be produced by prolonged exposure to air above that temperature. Since these materials were developed to be actuated by light, a more quantitative measure of their clarity was in order. UV/VIS spectroscopy was carried on the sample A1, both neat and with dissolved dye (Epolight™ 4121) at concentrations up to 110 ppm by weight. The measured absorption coefficients are shown

in Figure 2 at various dye levels from 500 to 900 nm wavelength. Also inset is shown the linear

dependence of absorption coefficient on dye concentration at 810 nm.   Without dye the material

has very low absorption and would be capable of transmitting light with low loss for distances on

the order of several centimeters. In previous work [34] it was demonstrated that an SMP fiber 200

microns in diameter was cable of transmitting 8 Watts of laser energy (at 810 nm) for 2 minutes

without degrading. At the same time, the addition of dye should allow for the controlled thermal

actuation of devices made from these materials in sizes ranging from hundreds of microns to tens of

centimeters.

DSC Results.

DSC thermograms for the A, B, and C series of SMPs are seen in Figures 3 to 5, and

summarized in Table 2. First heating scan, not shown, display single glass transition steps and no

indication of a reaction exotherm, supporting the solvent extraction and NMR data for a very high

level of conversion. In Figures 3 to 5 the 2nd heating cycle results are shown for series A, B, and C

compositions. It be seen that the polymers exhibit essentially a single step transition, i.e. a single

glass transition, indicating an amorphous network structure.   This view is supported by both the

optical clarity of the materials as well as the DMTA data which will be presented in the next

section. The glass transition temperatures (Tg) are likewise directly tied to the composition of each

material and were found to be well modelled using a generalized form of the Fox [35] equation:

$$1/T_g = \sum w_i / T_{g,i}$$

where w_i and $T_{g,i}$ are the weight fractions and glass transitions of monomer i, respectively. This

further supports the view that these SMPs are a single phase amorphous system. Glass transition

results for pure copolymers of HMDI and IPDI with HPED were found to be 153.8 and 145.3 ºC,

respectively. This dramatic increase in T_g versus the HDI based polymer can be attributed to the cyclic structures in the network chain backbones increasing chain stiffness and reducing the chain mobility [26].

Results by DMTA.

DMTA tests were run on the new SMPs in order to both determine mechanical glass transition temperatures as well as shear elastic moduli (G') in the polymers above the glass transition. Values of G' are directly related to the Young's modulus in elastomeric materials (E ≈ 3G') and should therefore directly relate to recovery forces exerted by the material during shape recovery. DMTA results (G' and tanδ) are shown for the urethane series A, B, and C in Figures 6 through 8. Using Figure 6 as an example, it can be seen that at low temperature the SMPs have moduli in the range of glassy polymers, at higher temperatures the modulus goes through a sharp transition, dropping about 2 orders in magnitude over about 20 ºC. At the highest temperatures shown the modulus is in the range of fairly stiff elastomers and increases slightly with temperature. The curves for tanδ likewise indicate a single sharp transition with values that rapidly go below the instrument resolution above the material T_g. This type of behavior is consistent with the hypothesis of a network polymer having an amorphous structure and very uniform network chain molecular weight and structure between crosslink sites. The very low values of tanδ in the region of rubbery behavior likewise indicate a very low amount of dangling chains and/or dangling groups with very low molecular weight such that their contribution to internal friction in the material during deformation is negligible compared to the elastic response in the material. The increase in modulus with temperature is predicted by statistical theories for flexible chain dynamics [25,36].

The temperatures of the tanδ peak, values of the shear elastic moduli measured at $T_g \pm 20$

ºC, and their ratio are given in Table 2. The peak in tanδ is often used as a measure of the glass transition temperature. In comparison with DSC, values are often found to be a few degrees higher and reflect the difference both in test procedure between DSC and DMTA, as well as inherent differences in chain dynamics sampled by the two techniques. For example, DSC values represent more localized chain motion which is enabled at lower temperatures. It can be seen in the data that the T_g values determined by DMTA systematically depend on composition in the same manner as those from DSC.

The ratio of G' in the glassy state versus the rubbery state, defined as $(G'(T_g-20ºC)/G'(T_g+20ºC))$, has been used as an indicator of the ability of an SMP to retain it's secondary shape and to recover its primary shape on acutation [37]. Generally, it is believed values in excess of 100 are necessary for good "shape memory" behavior. It can be seen that essentially every polymer formulation presented satifies this criteria. Additionally, the rubber plateau moduli of these materials, the sharp T_g's, and low tanδ's indicate the materials actuation can be very fast compared to previous SMP materials [19,38, 39]. Indeed, benchtop testing of devices 0.5 mm in thickness indicates full shape recovery in approximately 1 second compared to times on the order of tens of seconds for previously reported materials.

The effect of increasing the molecular weight between network junction points (crosslinks) can be seen with series B results in Figure 7. As the molecular weight between crosslinks increases (higher BD content), the elastic modulus above T_g decreases. Again, this is consistent with theories relating rubber modulus to crosslink density. On the other hand, adding methyl side groups to the polymer network chains as shown in Figure 8 (see series A versus C, Table 2) has the effect of reducing the modulus values (small decrease) while increasing the values of the T_g. These effects are presumably due to a decrease in the material density and density of active network chains, while

at the same time the side groups increase the stiffness of network chains and thereby increase T_g.

Tensile test results.

Tensile testing was carried out on a small subset of samples to determine the elastic modulus and extensibility of the SMP at temperatures above the glass transition, in turn helping to determine their suitability for device applications. Additionally, Young's modulus measured by tensile tensile testing was compared to G' as measured by DMTA.   In Figure 9 is shown a representative result for the neat A7/8 composition (Tg=53 ºC) and with the addition of 1 weight % of amine functionalized single walled nanotubes (SWNTs). First, Young's modulus values obtained from the data are in the range of 25 MPa, which was found to match 3G', as predicted for an ideal elastomer. This finding and the relative ease of running DMTA experiments versus tensile tests was used to justify limiting tensile testing and use of G' values to predict recovery stresses for shape memory behavior in these new materials. The extensibility of the SMP is also demonstrated to be at least 35% in strain, which is on the order of 5 times greater than that obtainable with shape memory alloys. These results place the new urethane SMPs in the target range for modulus intermediate between commercial SMPs (e.g. Mitsubishi's segmented urethanes) and SMAs. Turning to the effect of the addition of SWNTs, it can be seen in Figure 9 that the addition of a small weight fraction of SWNTs can increase both the modulus of the polymer and the extensibility (strength) of the material. It should be noted that the SWNT/polymer composite shown had indications that the SWNTs were not fully dispersed, as evidenced by up to 5 micron sized particulates seen via optical microscopy. Thus it is believed that further enhancement in properties can be obtained.

Results of cyclic tensile testing.

Cycle tensile testing was also run on select SMP formulations at temperatures 25 °C above their Tg's in order to evaluate the level of strain recovery that can be expected in the materials in shape memory applications. Representative results for the A7/8 formulation are shown for a test in which 20% engineering strain is linearly applied and then removed, with five total cycles shown. It can be seen that there is some initial hysteresis in the first cycle, which is presumably due to residual stress in the material as well as the re-arrangement of dangling chains and side-groups in the polymer. For cycles 2 through 5, almost no hysteresis is seen in the material with recoverable strains of 98 to 100%. In other words, the polymer behaves as a nearly ideal spring. These results are expected based on the extremely low values of tanδ measured for these materials and further support the extensive use of DMTA testing in evaluating these materials.

DISCUSSION

The first objective of this work was the development of new amorphous SMPs with a highly uniform network structure consisting of network chains with very similar molecular weight and composition between junction points. While the monomers chosen in this work were nominally suitable for this task, concerns could be raise regarding structure due to incomplete reaction (hence dangling chains) since such a tight network as designed here would be assumed to limit the ultimate extent of reaction that can be obtained. Surprisingly, solvent extraction and NMR results point to an extent of reaction within experimental error of 100%. Furthermore, mechanical testing by both DMTA and cyclic tensile show these materials to have very low mechanical hysteresis (loss), which likewise would indicate a relatively low level of pendent groups in the chain structure.

Additional information about the likely chain structure can be inferred from the values of the elastic modulus of the materials well above their glass transitions. Values of G' in the

HDI/HPED/TEA series of polymers range from approximately 5 to 7 MPa, corresponding to Young's moduli from 15 to 21 MPa. At the same time, assuming an idealized network structure the number of network chain atoms between junction points is 15 for HDI/HPED networks and 17 for HDI/TEA networks. It is interesting to compare these results to a material such as poly(ethylene) (PE). PE has entanglement molecular weight (M_e) of 1250 and a rubber plateau shear modulus of 2.3 MPa ($G°_N = 1/ J°_N$ where $J°_N$ is the shear compliance due to entanglements) [25]. A poly(ethylene) material with network chains of 15 carbons could then be calculated to have a plateau modulus of $G = G°_N * Me/Mc$ (= 2.3 * 1250/(28*15) = 6.8 MPa). The measured moduli for the new SMPs appear then to match well what might be expected for ideal networks based on simple analogies to linear flexible chain polymers. Also, the high values of modulus measured suggest a very low number of dangling chain loops that could form by reaction of the diisocyanate with two sites on a single polyol molecule, in contrast to the prediction of roughly 5% inactive chain loops calculated by Lee [40] for similar networks comprised of poly(oxypropylene) triols and tetrols. Collectively, these results make a strong case for the achievement of materials with very uniform networks.

CONCLUSIONS

1. New urethane network polymers were synthesized and characterized based on HDI, TMHDI, IPDI, HMDI, HPED, TEA, and BD monomers. Analysis of the materials indicates essentially full conversion of initial functional groups in the monomer formulations. These new polyurethanes were found to have an amorphous and but highly uniform network chain structure, displaying a single glass transition with very narrow breadth and very low mechanical loss above the glass transition.

2. The glass transition temperature and rubber plateau modulus of the new polymers can be readily controlled by varying the composition of the polymers, with Tg's measured ranging from 34 to 153 °C and shear moduli from 3 to 7 MPa.

3. The new urethane networks have thermo-mechanical properties which indicate they should have excellent shape memory behavior; namely, sharp glass transitions, a high glass to rubber modulus ratio, high rubber modulus, and low mechanical loss. Cyclic tensile testing as well as construction and testing of microdevices (to be published elsewhere) confirms this assessment. We believe these polymers represent a new and potentially important class of SMPs.

4. The new urethane SMPs have excellent optical clarity and can be dyed to control their absorption of light. This makes them especially promising for use in photo-thermally actuated SMP devices.

References

1. Tey, S. J., Huang, W. M., and Sokolowski, W. J., Smart Mater Struct, 2001, 10, 321-325.
2. Benett, W. J., Krulevitch, P. A., Lee, A. P., Northrup, M. A., and Folta. J. A., U.S. Patent No. 5783130, 1998.

3. Metzger, M., Wilson, T. S., Schumann, D. L., Matthews, D. L, and Maitland, D. J., Biomedical Microdevices, 2002, 4:2, 89.
4. Irie, M, In Shape Memory Materials, Otsuka, K. and C. M .Wayman, C. L. Ed.; Cambridge Univ. Press, Cambridge, 1998, Chap. 9.
5. Ishii, M., Zairyo Gijutsu (Jpn.) 1989, 7, 183.
6. Hayashi, S. and Shirai, Y., Mitsubishi Technical Bulletin No. 184, December 1988.
7. Anonomous, "Mitsubishi Shape Memory Polymer," Mitsubishi Heavy Industries, Ltd., April 2, 1992.
8. Tobushi, H. S., Hayashi, S., and Kojima, S., JSME Int Journal, 1993, 1 (3), 35.
9. Hayashi, S., Kondo, S., and Giordano, C., Proc SPE ANTEC, 1994, 1998.
10. Kim, B. K., Lee, S. Y., and Xu, M.., Polymer, 1996, 37 (26), 5781.
11. Kim, B. K., Lee, S. Y., Lee, J. S. , Baek, S. H., Choi, Y. J., J. O. Lee, J. O., and Xu, M., Polymer, 1998, 39(13), 2803.
12. Takahashi, T., Hayashi, N., and Hayashi, S., J Appl Pol Sci, 1996, 60, 1061.
13. Li, F., Zhang, X., Hou, J., Xu, M., X. Luo, X., Ma, D., and Kim, B. K., J Appl Pol Sci, 1997, 64, 1511.
14. Lin, J. R. and Chen, L. W., J Appl Pol Sci, 1998, 69, 1563; J Appl Pol Sci, 1998, 69, 1575.
15. Luo, X., Zhang, X., Wang, M., Ma, D., Xu, M., and Li, F., J Appl Pol Sci, 1997, 64, 2433.
16. Wang, W., and Zhang, L., J Pol Sci B: Pol Phys, 1999, 37(2), 101.
17. Li, F., Zhu, W. Zhang, X.., Zhao, C., and Xu, M., J Appl Pol Sci, 1999, 71, 1063.
18. Sakurai, K., Tanaka, H., Ogawa, N., and Takahashi, T., J Macromoleular Science-Physics, 1997, 36 (6), 703-716.
19. Lendlein, A., and Kelch, S., Angew Chem Int Ed, 2002, 41, 2034-2057.
20. Ward R. S., and J.S. Riffle, J. S., Patent WO 86/03980, July 17, 1986.
21. Kusy R. P., and Whitley, J. Q., Thermochimica Acta 1994, 243 (2): 253-263.
22. Dotter, C. T., Buschmann, R. W., McKinney, M. K., and Rosch, J., Radiology, 1983, 147 (1): 259-260.
23. Kornbluh, R., Pelrine, R., Shastri, S. V., Full, R. J., Meijer, K., SRI Report Number 433-PA-00-013, Menlo Park, CA.
24. Liu, C., and Mather, P.T., "Thermomechanical Characterization of a Novel Series of Shape Memory Polymers," SPE ANTEC Proceedings (2002).
25. Ferry, J. D., Viscoelastic Properties of Polymers, 3rd ed., Wiley and Sons, New York, 1980.
26. Shaw, M.T. and McKnight, W.J., Introduction to Polymer Viscoelasticity, 3rd ed., Wiley Interscience, New York, 2005.
27. Lamba, N.M.K., Woodhouse, K.A and Cooper, S. L., Polyurethanes in Biomedical Applications, CRC Press, New York, 1997.
28. Marks, D., and Vega, S., Journal of Magnetic Resonance, Series A, 1996, 118, 157-172.
29. Pyris© Thermal Analysis Software, Perkin Elmer Life and Analytical Sciences Inc., Wellesley, MA.
30. Wunderlich, B., J Thermal Analysis, 1996, 46 (3-4): 643-679 MAR-APR.
31. Orchestrator ver. 6.6.0, TA Instruments Inc., Wilmington DE, 2004.
32. JL Koenig, Chemical Microstructure of Polymer Chains, Wiley-Interscience, New York, 1980, 378.
33. Rethwisch, D. G., Jacintha, M. A., and Dybowski, D. R., Analytica Chimica Acta, 1993, 283, 1033-1043.
34. Wilson, T.S., Small IV, W., Benett, W. J., Bearinger, J. P., and Maitland, D. J., Proc SPIE, 2005, Vol 6007, pp. 157-164.
35. Fox, T. G., Bull Am Phys Soc, 1956, 1, 123.
36. Sperling, L. H., Introduction to Physical Polymer Science, 3rd ed., Wiley Interscience, New York, 2001.
37. Hayashi, S., Int Prog Urethane, 1993, 6, 90.
38. A. Lendlein, A. Schmidt, and R. Langer, Proc. Nat. Acad. Sci., 98(3), 842-847, 2001.
39. Gall, K., Dunn, M. L., Liu, Y., Finch, D., Lake, M., and Mushi, N. A., Acta Materials, 2002, 50, 5115.
40. Lee, K. J. and Eichinger, B. E., Polymer, 1990, 31(3), 406.

List of Figures Captions:

Figure 1. Solid state ^{13}C CPMAS NMR of HDI and HPED copolymers. The upper curve is for an HDI/HPED molar ratio of 1:1 with an NCO/OH ratio of 0.5, while the bottom curve is for a molar ratio of 2:1 with an NCO/OH ratio of 1.0 (stoichiometric).

Figure 2. UV/VIS spectra of A1 polymer, neat and with varying levels of Epolight™ 4121 dye.

Figure 3.   DSC thermograms of 2nd heating cycle for HDI/HPED/TEA series copolymers A1 through A11. Curves have been shifted vertically to allow for comparison.

Figure 4. DSC thermograms of 2nd heating cycle for HDI/HPED/1,3BD series copolymers B1-B7. Curves have been shifted vertically to allow for comparison.

Figure 5. DSC thermograms of 2nd heating cycle for TMHDI/HPED/TEA series copolymers C1-C6. Curves have been shifted vertically to allow for comparison.

Figure 6. (a)Dynamic shear storage modulus (G') and (b) tan(delta) from DMTA temperature sweeps on HDI/HPED/TEA series (A1-11) polymers.

Figure 7. (a)Dynamic shear storage modulus (G') and (b) tan(delta) from DMTA temperature sweeps on HDI/HPED/1,3BD series (B1, B3, B5, B7) polymers.

Figure 8. (a)Dynamic shear storage modulus (G') and (b) tan(delta) from DMTA temperature sweeps on TMHDI/HPED/TEA series (C1-C6) polymers.

Figure 9. Tensile modulus of neat A7/8 formulation and with 1 weight % added amine-functionalized single walled carbon nanotubes at 80 ºC.

Figure 10. Cyclic tensile testing of neat A7/8 formulation to 20% engineering strain at 80 ºC. Five cycles are shown.

Table 1. Relation of SMP Morphology to Optical and Actuation Properties

| Polymer System	Matrix Phase	Fixing Phase	Actuation Transition	Transition Breadth	Recovery Forces	Optical Properties
Amorphous (linear)	amorphous chains	entanglements	T_g	sharp to broad	low	clear
Amorphous (crosslinked)	amorphous chains	crosslinks	T_g	sharp to broad	low to high	clear
Semicrystalline (linear)	amorphous chains	crystalline phase	T_g	very sharp to broad	low to high	turbid below Tm
Semicrystalline (crosslinked)	amorphous chains	crystalline phase or crosslinks	T_g or T_m	very sharp to broad	low to high	turbid below Tm
Block copolymer (incompatible blocks), (linear)	amorphous soft phase	amorphous hard phase, crystals in soft phase, crystals in hard phase,	$T_{g,s}$ $T_{m,s}$	sharp to broad	low to high	translucent to turbid
Block copolymer (incompatible blocks), (crosslinked)	amorphous soft phase, amorphous hard phase	amorphous hard phase, crystals in soft phase, crystals in hard phase, crosslinks	$T_{g,s}$ $T_{m,s}$ $T_{g,h}$ $T_{m,h}$	sharp to broad	low to high	translucent to turbid

Table 2. Molar Composition and Thermal/Mechanical Transitions of Urethane Network SMPs

Polymer Designation	HDI (f=2) moles	TMHDI (f=2) moles	HPED (f=4) moles	TEA (f=3) moles	1,3 BD (f=2) moles	T_g (DSC) (°C)	Degree of Gelation %	T_g (G") (°C)	T_g (tanδ) (°C)	G' at T_g+20 (MPa)	G' Ratio
A1	1.00	-	0.50	0.000	-	86.4	97.7	80.1	88.3	7.2	97
A2	1.00		0.45	0.067		82.9	-	77.7	86.6	6.9	104
A3	1.00	-	0.40	0.133	-	75.7	-	71.6	80.7	7.1	102
A4	1.00		0.35	0.200		70.8	-	69.8	78.2	7.0	104
A5	1.00	-	0.30	0.267	-	66.4	-	65.1	74.7	7.0	115
A6	1.00		0.25	0.333		60.4	-	60.3	69.5	6.8	120
A7	1.00	-	0.20	0.400	-	56.1	-	55.6	64.0	6.6	137
A8	1.00		0.15	0.467		50.7	-	49.7	58.7	6.2	152
A9	1.00	-	0.10	0.533	-	43.3	-	43.2	51.3	5.7	148
A10	1.00		0.05	0.600		38.4	-	37.7	45.3	5.3	-
A11	1.00	-	0.00	0.667	-	33.8	96.1	33.5	40.7	5.2	-
B1=A1	1.00	-	0.50	-	0.00	86.2	-	80.1	88.3	7.1	99
B2	1.00	-	0.45	-	0.10	81.3	-	78.0	86.6	6.8	104
B3	1.00	-	0.40	-	0.20	76.4	-	72.5	81.1	6.0	122
B4	1.00	-	0.35	-	0.30	71.7	-	63.2	71.8	4.8	167
B5	1.00	-	0.30	-	0.40	67.0	-	63.7	72.5	4.7	164
B6	1.00	-	0.25	-	0.50	61.6	-	59.8	69.1	4.0	192
B7	1.00	-	0.20	-	0.60	57.5	96.3	51.7	60.9	3.1	280
C1	-	1.00	0.50	0.000	-	89.8	98.8	84.2	92.2	5.3	143
C2	-	1.00	0.40	0.133	-	81.8	-	76.3	84.7	4.9	148
C3	-	1.00	0.30	0.267	-	72.1	-	68.9	77.2	4.7	176
C4	-	1.00	0.20	0.400	-	64.1	-	61.0	70.0	4.5	201
C5	-	1.00	0.10	0.533	-	56.0	-	53.6	61.9	4.2	230
C6	-	1.00	0.00	0.667	-	44.8	-	42.2	49.2	4.3	243

Table 3. Elemental Composition (atomic %) of Shape Memory Polymers

Sample	C 1s	N 1s	O 1s
03	72.97	7.38	19.65
04	72.40	9.78	17.80
05	73.11	8.97	17.93

HDI/HPED = 1:1 molar

HDI/HPED = 2:1 molar
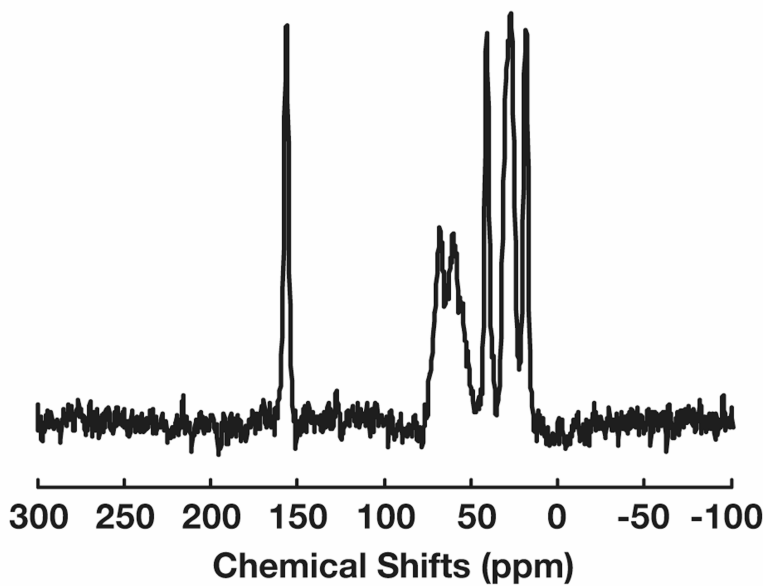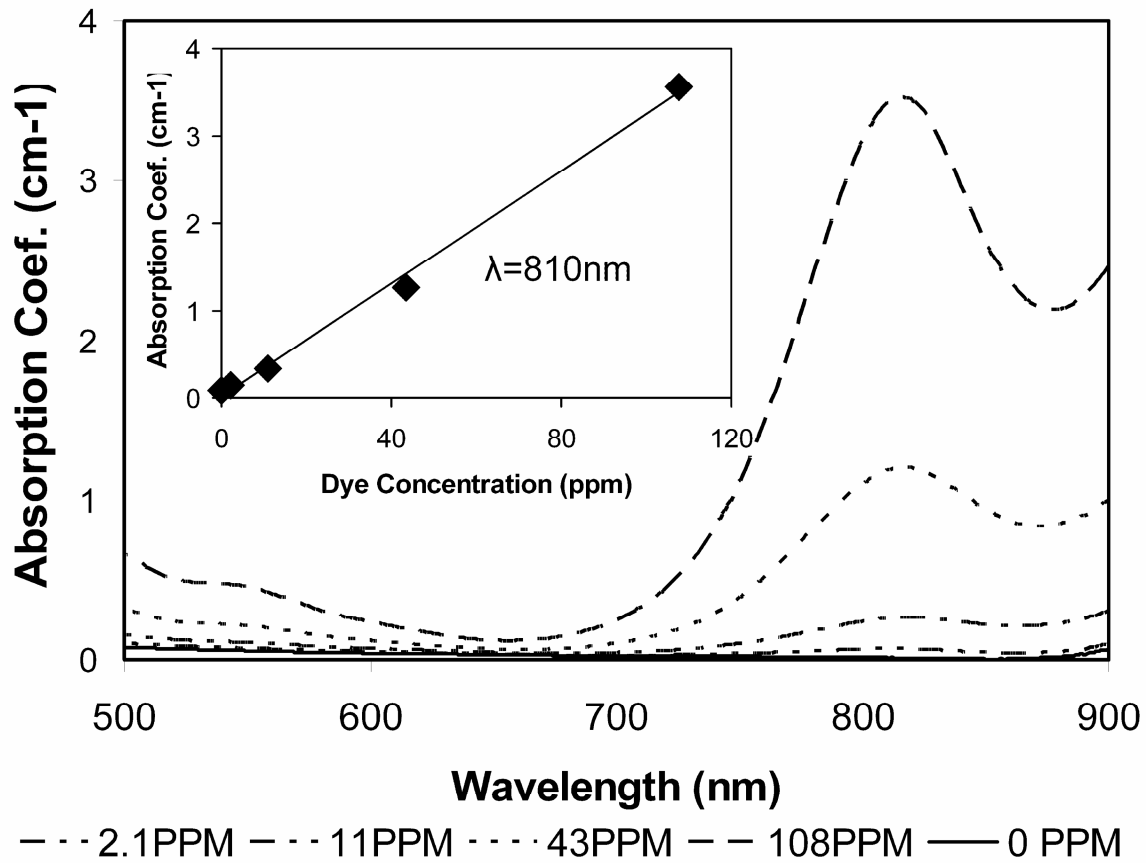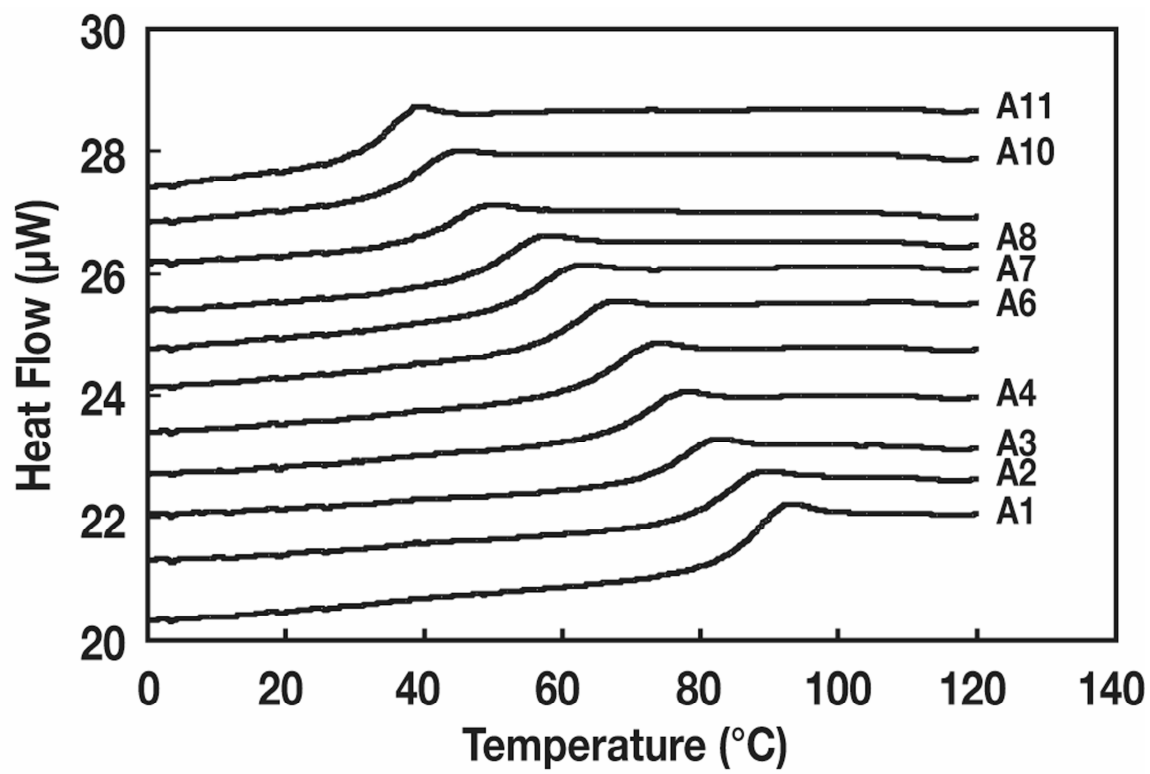
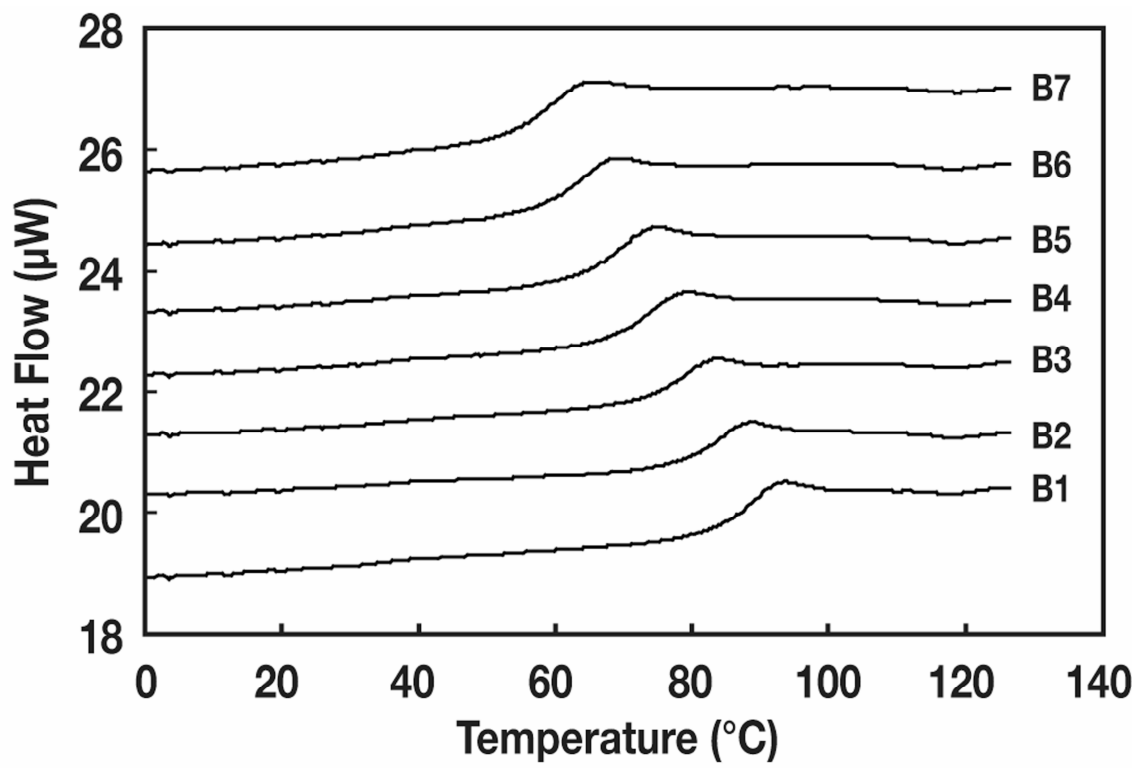300   250   200   150   100   50   0   -50   -100
Chemical Shifts (ppm)
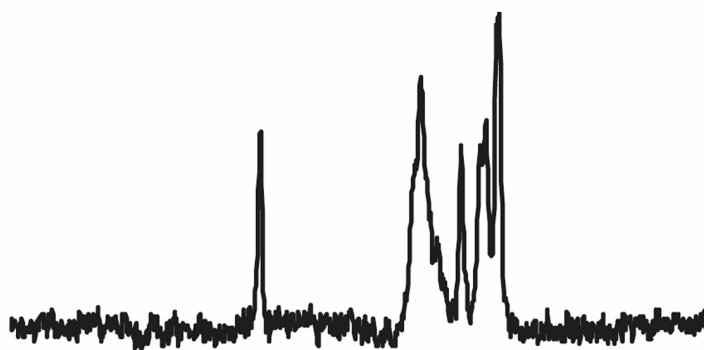
Figure 1

Figure 2

Figure 3

Figure 4

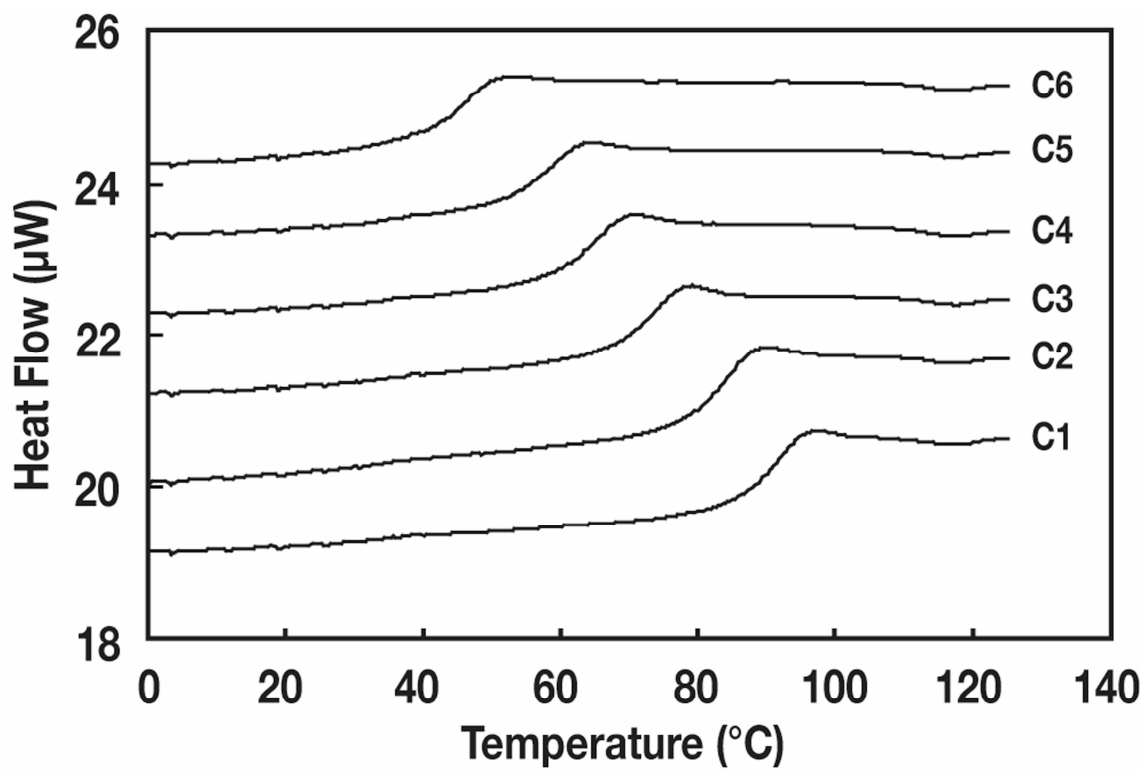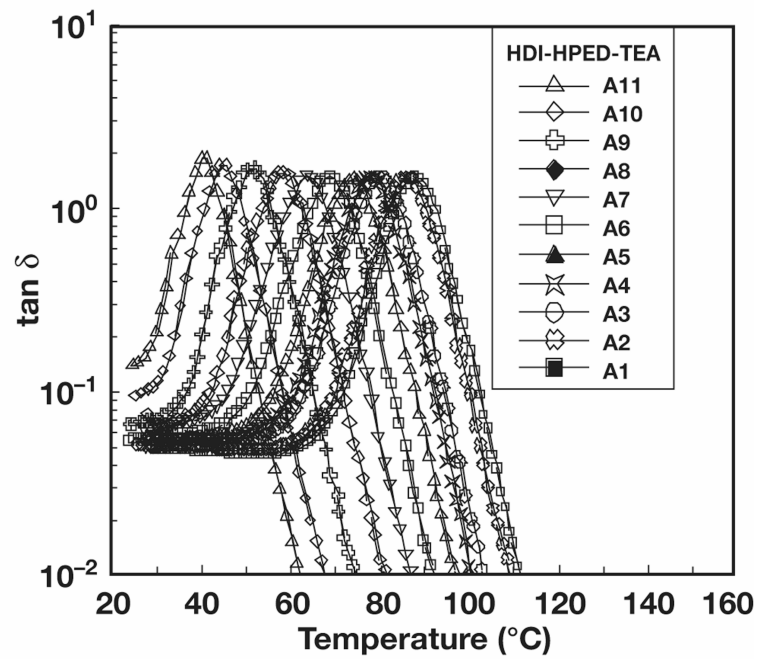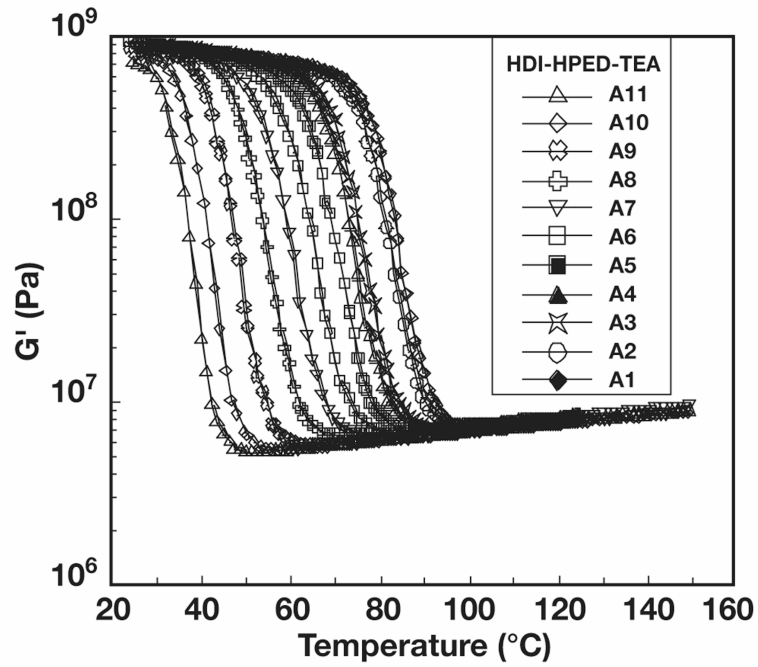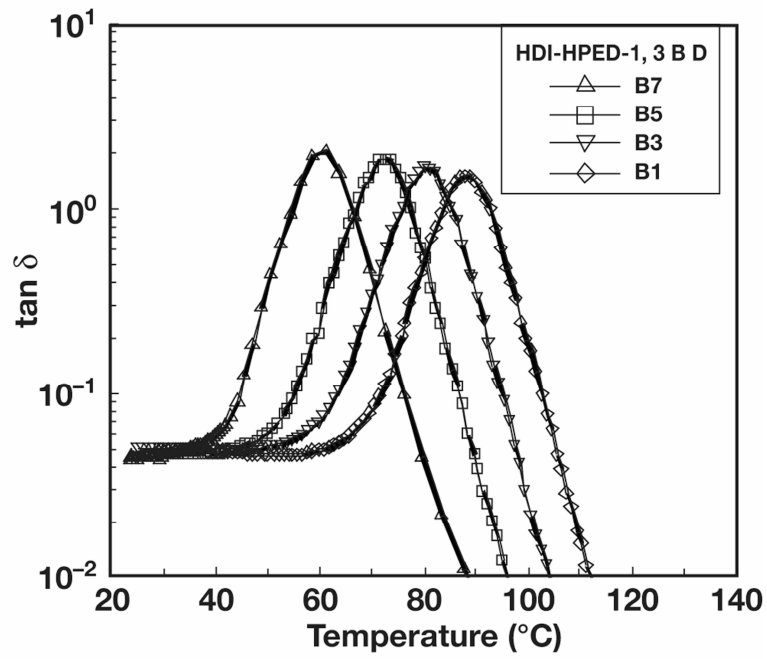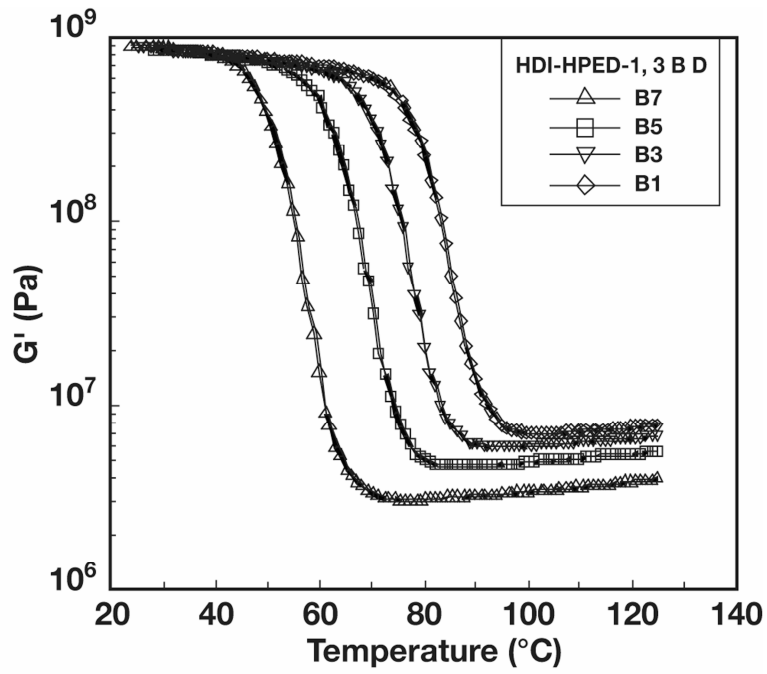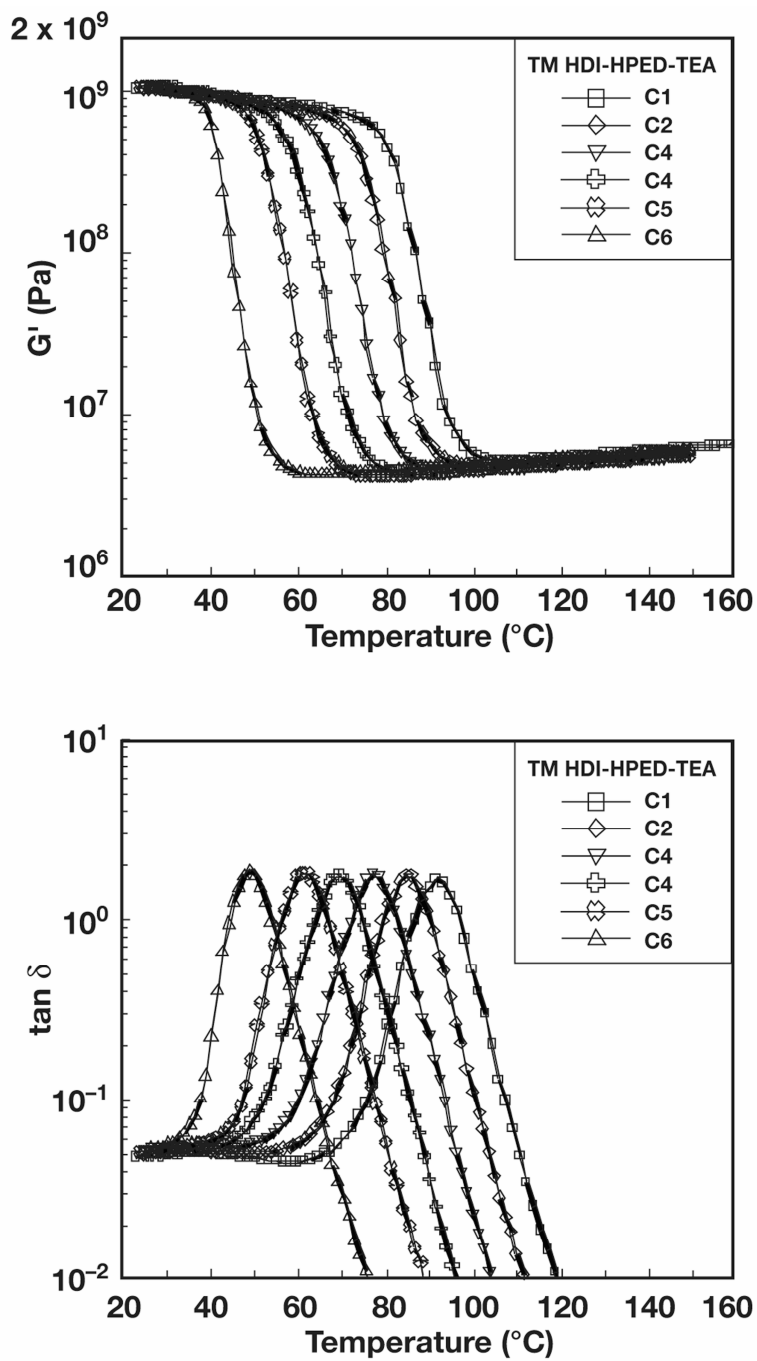Figure 5

Figure 6

Figure 7

Figure 8

Figure 9

Figure 10